IOPscience iopscience.iop.org

Home Search Collections Journals About Contact us My IOPscience

Materials science and fabrication processes for a new MEMS technology based on ultrananocrystalline diamond thin films

This article has been downloaded from IOPscience. Please scroll down to see the full text article.

2004 J. Phys.: Condens. Matter 16 R539

(http://iopscience.iop.org/0953-8984/16/16/R02)

View the table of contents for this issue, or go to the journal homepage for more

Download details:
IP Address: 129.252.86.83
The article was downloaded on 27/05/2010 at 14:26

Please note that terms and conditions apply.

INSTITUTE OF PHYSICS PUBLISHING JOURNAL OF PHYSICS: CONDENSED MATTER

J. Phys.: Condens. Matter **16** (2004) R539–R552 PII: S0953-8984(04)56693-6

TOPICAL REVIEW

Materials science and fabrication processes for a new MEMS technology based on ultrananocrystalline diamond thin films

Orlando Auciello[1], James Birrell[1], John A Carlisle[1], Jennifer E Gerbi[1], Xingcheng Xiao[1], Bei Peng[2] and Horacio D Espinosa[2]

[1] Argonne National Laboratory, Materials Science Division, 9700 South Cass Avenue, Argonne, IL 60439, USA

[2] Department of Mechanical Engineering, Northwestern University, Evanston, IL 60208-3111, USA

Received 20 January 2004
Published 8 April 2004
Online at stacks.iop.org/JPhysCM/16/R539
DOI: 10.1088/0953-8984/16/16/R02

Abstract

Most MEMS devices are currently based on silicon because of the available surface machining technology. However, Si has poor mechanical and tribological properties which makes it difficult to produce high performance Si based MEMS devices that could work reliably, particularly in harsh environments; diamond, as a superhard material with high mechanical strength, exceptional chemical inertness, outstanding thermal stability and superior tribological performance, could be an ideal material for MEMS. A key challenge for diamond MEMS is the integration of diamond films with other materials. Conventional CVD thin film deposition methods produce diamond films with large grains, high internal stress, poor intergranular adhesion and very rough surfaces, and are consequently ill-suited for MEMS applications. Diamond-like films offer an alternative, but are deposited using physical vapour deposition methods unsuitable for conformal deposition on high aspect ratio features, and generally they do not exhibit the outstanding mechanical properties of diamond. We describe a new ultrananocrystalline diamond (UNCD) film technology based on a microwave plasma technique using argon plasma chemistries that produce UNCD films with morphological and mechanical properties that are ideally suited for producing reliable MEMS devices. We have developed lithographic techniques for the fabrication of UNCD MEMS components, including cantilevers and multilevel devices, acting as precursors to micro-bearings and gears, making UNCD a promising material for the development of high performance MEMS devices. We also review the mechanical, tribological, electronic transport, chemical and biocompatibility properties of UNCD, which make this an ideal material for reliable, long endurance MEMS device use.

(Some figures in this article are in colour only in the electronic version)

Contents

1. Si as a MEMS material 540
2. Single-crystal diamond, microcrystalline diamond (MCD), and ultrananocrystalline diamond (UNCD) films as MEMS materials 541
3. Alternative growth processes for production of diamond films for MEMS 542
   3.1. Methyl radical growth processes for microcrystalline and nanocrystalline diamond films 542
   3.2. Ar-rich CH_4/Ar microwave plasma growth process for ultrananocrystalline diamond (UNCD) films 542
4. Fabrication processes for MEMS based on UNCD 544
   4.1. Conformal diamond coating 544
   4.2. Selective deposition 545
   4.3. Lithographic patterning 545
5. Measurement of mechanical properties of UNCD at the MEMS scale 547
   5.1. Membrane deflection experiment 547
   5.2. Microcantilever deflection experiments 550
   5.3. Tribological behaviour of UNCD 550
6. Other properties of UNCD relevant to MEMS 550
7. Conclusions 551

   Acknowledgments 551

   References 551

1. Si as a MEMS material

The development of methods for the production of miniaturized mechanical components and devices in Si is a natural outgrowth of the Si surface machining methods that have been developed for the production of microcircuits. Complex shapes, such as levers, gears and pinwheels [1], have been produced using standard lithographic patterning and etch methods, and fully assembled devices such as micromotors and gear-trains have been produced using multiple masks and multilayer deposition and etching techniques [1]. Unfortunately, Si has poor mechanical and tribological properties [2, 3], and practical MEMS devices typically must be designed to circumvent these limitations [4]. In particular, it is common practice to avoid extensive sliding and rolling contact, and to minimize the flexural stress required of torsion bars and cantilevers. The poor brittle fracture strength of Si and the tendency of Si to adhere to surfaces with which it makes contact limit the degree of flex that a Si cantilever can undergo, and also rule out the use of motion limit structures to prevent cantilever breakage under high load conditions. Consequently, cantilever acceleration sensors used as automotive airbag actuators are designed as limited range threshold detectors, rather than wide range measuring devices. Rotating devices such as pinwheels [3] and microturbines [5] have been fabricated, but are frequently subject to stiction problems that prevent start-up [1], or wear-related failure after a few minutes of operation [2]. In order to be able to realize the full potential of MEMS, it will be necessary to produce MEMS devices that survive under conditions of significant rolling and sliding contact under extreme environmental conditions. One approach to controlling stiction issues in silicon devices is to modify the surface chemistry of silicon, through the use of anti-stiction coatings (self-assembled monolayers and the like), but these coatings are not suitable for all applications and in general greatly add to the cost of packaging of the devices. SiC has been proposed as an alternative material, especially for MEMS applications that involve high temperature oxidizing environments [6]. However, SiC has its own tribological shortcomings [7] and the fabrication methods are limited [8].

Table 1. Selected mechanical properties of Si, SiC and diamond.

Property	Silicon	Silicon carbide	Diamond
Cohesive energy (eV)	4.64	6.34	7.36
Young's modulus (GPa)	130	450	1200
Shear modulus (GPa)	80	149	577
Hardness (kg mm^{-2})	1000	3500	10 000
Fracture toughness	1	5.2	5.3
Flexural strength (MPa)	127.6	670	2944

2. Single-crystal diamond, microcrystalline diamond (MCD), and ultrananocrystalline diamond (UNCD) films as MEMS materials

Diamond is an ultrahard material with high mechanical strength, exceptional chemical inertness and outstanding thermal stability among other properties. Relevant mechanical properties of Si, SiC and diamond are shown in table 1.

The coefficient of friction (COF) of single-crystal diamond is exceptionally low (0.02–0.01), and the projected wear life is 10 000 times greater than that of Si, making diamond, in principle, an ideal tribomaterial for MEMS components [4, 9]. A low COF is important since lubrication is one of the major limitations on the design of MEMS devices because the usual methods of delivering lubricant to the interface between contacting parts are very difficult to implement. Additionally, the viscosity of liquid lubricants is sufficient to prevent motion of MEMS components. The lubrication problem is in principle solved by diamond since its surface is naturally hydrogen or oxygen terminated providing a natural lubricant. However, single-crystal diamond is not suitable for fabrication of MEMS devices because it is expensive and it cannot be processed in a cost efficient manner using the microfabrication methods utilized for production of Si based MEMS.

In relation to the suitability of non-Si materials for harsh environment MEMS, in high temperature oxidizing atmospheres one would expect Si or SiC to be the superior material, since they form a refractory oxide, whereas diamond burns in oxygen. For relatively low oxygen partial pressures however, diamond exhibits friction and wear coefficients that are considerably lower than those of Si and SiC, even at temperatures in excess of 900 °C [9]. Pin-on-disc tribometer measurements of the COF of Si, SiC, mechanically polished MCD films and UNCD films during a temperature ramp to 900–950 °C in an oxygen atmosphere of 3.4 Torr showed that the COF of Si has a relatively high and constant value of 0.6 throughout that temperature range, whereas the COF of MCD and UNCD starts at 0.05 at room temperature and drops to 0.01–0.02 as the temperature increases [10]. This behaviour has been tentatively ascribed [9] to the formation of a stable adsorbed oxygen moiety on the diamond surface that saturates the diamond dangling bonds and therefore minimizes bonding between contacting diamond surfaces. SiC exhibits a behaviour that is intermediate between that of Si and diamond in that the friction coefficient is high (0.5) at room temperature, and then drops to a value of 0.2 as the temperature exceeds 200 °C. This behaviour is consistent with a linear superposition of the friction of separate Si and carbon surface phases. However, at room temperature in air, MCD and diamond-like carbon (DLC) films exhibit higher COF ($\sim$0.1) than UNCD ($\sim$0.02–0.03) [10]. In addition to the tribological properties measured at the macroscale, as described above, extensive macroscopic measurements revealed that UNCD exhibits a hardness (98 GPa) and Young modulus ($\sim$980 GPa) similar to those for single-crystal diamond [10]. All these properties were reviewed in a prior publication [10].

Macroscopic pin-on-disc tribometer measurements were performed to determine the COF of UNCD and MCD films using a SiC pin [11]. The COF depends on the surface roughness of the films. Therefore, it is not surprising that the COF of MCD films increased from 0.48 to 55.0 (10^{-6} mm^3 N^{-1}m^{-1}) as the film thickness increased from 2 to 10 μm, since the rms roughness increased from 95 to 376 nm. On the other hand, the COF for UNCD, in air, was about 0.03–0.04, independent of film thickness in the range 2–10 μm. The wear rate of the pin passed on the MCD film was $\sim 1 \times 10^{-6}$ mm^3 N^{-1}m^{-1}. For UNCD films the wear coefficient of the SiC pin ranged from $\sim$0.1 for short runs (8000 cycles) to 0.01 for a long run (2.2×10^6 cycles). A wear rate of 0.018×10^{-6} mm^3 N^{-1} m^{-1} was measured for a 6.0 μm thick UNCD film grown from a C_{60} carbon precursor. These measurements demonstrated that the as-grown UNCD films have wear coefficients roughly two orders of magnitude lower than those of MCD films of comparable thickness.

In this review, we present measurements of mechanical and tribological properties at the MEMS scale to provide evidence for the feasibility of using UNCD for a new reliable MEMS technology that is also suitable for harsh environments.

3. Alternative growth processes for production of diamond films for MEMS

3.1. Methyl radical growth processes for microcrystalline and nanocrystalline diamond films

The approach for fabrication of diamond MEMS will involve the synthesis of diamond films on an appropriate platform such as Si or metallic or insulating substrates, followed by surface micromachining processes as applied in the fabrication of Si MEMS. One alternative is to use conventional chemical vapour deposition (CVD) methods developed in the past that utilize hydrogen-rich CH_4/H_2 chemistry [12], where the principal growth species are CH_3^* radicals. Atomic hydrogen drives the hydrogen abstraction reactions that

(1) prepare the CH_3^* adsorption site by removing a hydrogen atom from the hydrogen terminated diamond surface and
(2) remove the hydrogen atoms from the adsorbed CH_3^*, thereby permitting the carbon atom to move into the position corresponding to the diamond lattice.

The atomic hydrogen is added to preferentially etch the graphitic phase. By using a plasma containing 98–99% H_2, it is possible to grow diamond films that are largely free of non-diamond secondary phases. However, atomic hydrogen also etches the diamond phase, resulting in the formation of intergranular voids and a columnar morphology with grain size and rms surface roughness typically $\sim$10% of the film thickness. The grain morphology is therefore not suited for the fabrication of MEMS components requiring resolution <1 μm.

The grain size can be reduced to 50–100 nm by increasing the CH_4/H_2 ratio in the plasma, which also results in a smoother film surface topography than for polycrystalline diamond films. However, intergranular non-diamond carbon phases are introduced into these diamond films. Consequently, the brittle fracture strength is limited by intergranular failure, and the mechanical properties of single-crystal diamond are not realized [13].

3.2. Ar-rich CH_4/Ar microwave plasma growth process for ultrananocrystalline diamond (UNCD) films

In the process described above, hydrogen abstraction reactions are needed in order to generate methyl radicals in the plasma as well as to remove hydrogen from the growing surface, so that

methyl radicals can chemisorb to it. In contrast, over the past few years we have developed a microwave plasma synthesis process that involves an argon-rich chemistry [14]. In this new plasma chemistry, a small amount of CH_4 (typically 1%) produces carbon dimers, C_2, which are derived from methane via the reactions

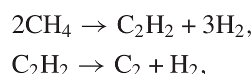

$$2CH_4 \rightarrow C_2H_2 + 3H_2,$$
$$C_2H_2 \rightarrow C_2 + H_2,$$

and are thought to play a critical role in the growth process although it is not clear yet whether the growth is mainly due to the C_2 dimers or whether there is a contribution also from hydrocarbon radicals in the plasma. We are currently investigating this issue. In any case, the distinctive characteristic of the new growth process is that the plasma contains very small quantities of hydrogen, arising mainly from the thermal decomposition of methane to acetylene in the plasma (about 1.5%). Typical deposition conditions for the 2.56 GHz microwave CVD reactor used in the growth of UNCD films are: 1% CH_4/99% Ar at a total flow rate of $\sim$100 sccm and a pressure of 100–200 Torr, and substrate temperatures ranging from 350 to 800 °C [15]. As a result of the limited amount of atomic hydrogen in the plasma, a very high renucleation rate ($\sim 10^{11}$ cm^{-2} s^{-1}) is maintained, resulting in a unique film microstructure consisting of equiaxed grains with a diameter of 3–5 nm [16]. The relative lack of atomic hydrogen in this process also minimizes re-gasification of these very small grains, thereby achieving a reasonably high linear growth rate and the formation of continuous films at very low thickness. We have demonstrated that UNCD films grow with rates in the range 0.2–0.4 μm h^{-1} in the 400–800 °C temperature range as measured by time of growth and cross-section SEM measurement of film thickness. UNCD is perhaps the only diamond material that grows at a reasonably high rate at temperatures as low as 400 °C. We performed extensive temperature calibration using a special commercial calibration wafer with 16 embedded thermocouples to make sure that the substrate temperatures are accurate. We have grown UNCD films as thick as 10 μm, but we have not tried to grow thicker films. In principle, we see no limitations on the film thickness that can be achieved within a useful range.

The nanometre-scale structure of UNCD is truly unique. UNCD consists of crystalline grains of pure sp^3 bonded carbon that are 3–5 nm in size, separated by *atomically abrupt* (0.5 nm wide), high energy grain boundaries. UV Raman spectroscopy [17] and synchrotron based near-edge x-ray absorption fine structure measurements [18] show the presence of about 5% sp^2 bonding in a typical UNCD film. The grain boundaries have been studied in detail [i] and consist of a mixture of sp^3, sp^2 and other types of bonding, and because of their local structure these high energy grain boundaries are much more mechanically stable compared to the low energy boundaries found in MCD [18]. The combination of large amounts of sp^3 bonded carbon and the local order of these bonds gives UNCD its unique materials properties. For instance, it is predicted that the brittle fracture strength of UNCD is equal to or greater than that of even perfect single-crystal diamond [19], and our recent measurements do indeed show fracture strengths of 4–5 GPa, as is discussed in detail in section 5.

UNCD exhibits a unique combination of properties that distinguish it from conventionally grown nanocrystalline diamond described in the previous section. We have therefore coined the term ‘ultrananocrystalline diamond’ (UNCD) (2–5 nm grain size) [10] to distinguish this material from microcrystalline diamond (MCD) (1–10 μm grain size) [20], nanocrystalline diamond (NCD) (50–100 nm grain size) [21] and high temperature stress-relieved diamond-like carbon (DLC) (amorphous) [21] which are being investigated as materials for fabricating MEMS components. The main characteristics of these materials are shown in table 2.

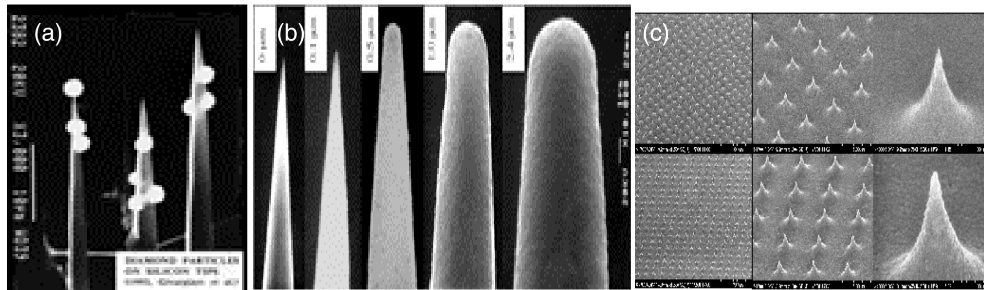

Figure 1. (a) High aspect ratio Si tips coated with MCD films; (b) high aspect ratio Si tips coated with UNCD films of various thickness; (c) a low aspect ratio Si tip array coated with UNCD film.

Table 2. Characteristics of diamond and diamond-like carbon (DLC) films.

				Diamond-like carbon	
	MCD	NCD	UNCD	ta-C	ta-H:C
Growth species	$CH_3^*(H^o)$	$CH_3^*(H^o)$	C_2	C	C
Crystallinity	Columnar	Mixed diamond & non-diamond	Equiaxed diamond	Mixed diamond & amorphous	Amorphous
Grain size	~0.5–10 μm	50–100 nm	2–5 nm	Variable	—
Surface roughness	400 nm–1 μm	50–100 nm	20–40 nm	5–100 nm	1–30 nm
Electronic bonding	sp^3	Up to 50% sp^2 (second phase)	2–5% sp^2 (in GB)	Up to 80% sp^3	Up to ~40% sp^3
Hydrogen content	<1%	<1%	<1%	<1%	15–60%

4. Fabrication processes for MEMS based on UNCD

There are a number of ways in which diamond components can be fabricated for MEMS applications using thin film deposition methods. Some of these are analogous to Si surface machining methods, and others have no counterpart in Si fabrication technology.

4.1. Conformal diamond coating

One of the more obvious methods of obtaining the tribological benefits of diamond while exploiting the availability of Si fabrication technology is to produce Si components to near-net shape and then provide a thin, low wear, low friction diamond coating [22, 23]. This approach only works if the diamond film can be produced as a thin, continuous, conformal coating with exceptional low roughness on the Si component. Conventional diamond CVD deposition methods result in discontinuous films with a low density of large grains and poor ability to form thin conformal coatings on Si microstructures (see figure 1(a) for example) [24]. On the other hand, UNCD films can coat high aspect ratio MEMS structures extremely conformally even for thick films, as shown for example by high and low aspect ratio UNCD-coated Si tips (figures 1(b) and (c)).

Although the tribological properties of UNCD-coated Si MEMS structure may be those of UNCD, the mechanical properties may be dominated by the Si core in this approach. Therefore, this is not the preferred approach for fabrication of MEMS based on UNCD films.

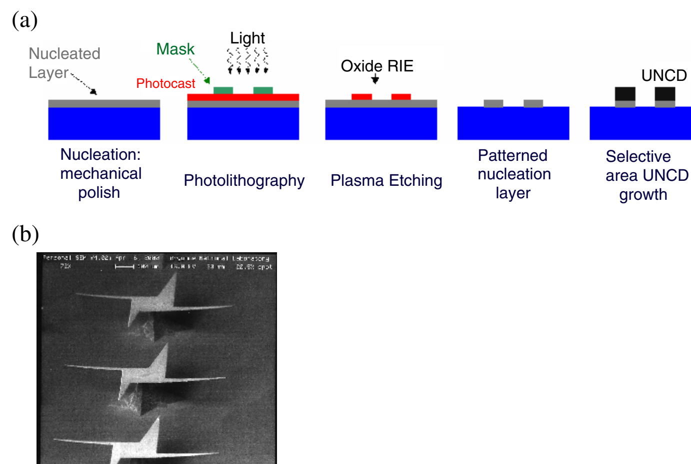

Figure 2. (a) A schematic diagram of a selective seeding and growth process used to produce UNCD MEMS structures; (b) an SEM picture of UNCD MEMS structures produced by selective seeding plus selective growth of UNCD plus selective etching of the Si substrate.

4.2. Selective deposition

Selective deposition represents a second method that may be used for the production of UNCD microstructures but has no analogue in Si microfabrication technology. All diamond films, including UNCD, require a nucleation layer, usually achieved by exposing the substrate to a suspension of fine diamond particles. It is possible to seed a selected portion of the substrate by (a) using photoresist to prevent exposure of selected areas to the diamond powder, (b) using diamond-loaded photoresist to produce a patterned nucleation layer or (c) seeding the substrate uniformly and then selectively etching portions of the surface to remove diamond-seeded areas. Alternatively, it is possible to use SiO_2 as a mask, since diamond films grown from CH_4–H_2 plasmas are normally unable to form on SiO_2 substrates. The feature resolution that can be achieved by this method is limited by the grain size [26]. An example of a selective UNCD growth process is shown in figure 2(a). A UNCD structure formed by selective seeding and growth followed by selective etching of the Si substrate is shown in figure 2(b).

The long arms ($\sim$1000 μm long) extending from the corners remain flat, proving that the UNCD film exhibits low stress (we have measured stresses in the range 50–100 MPa), unlike conventional diamond films that exhibit significant out-of-plane stress and consequent warping upon release from the substrate.

4.3. Lithographic patterning

In order to produce diamond multilayer structures, it is necessary to deposit a thin diamond film on a sacrificial release layer such as SiO_2. Methods have been reported [20] that force the growth of conventional CVD diamond on SiO_2, typically by damaging the SiO_2 surface by ultrasonic abrasion in a diamond powder suspension. Continuous diamond films have been achieved using this method for film thickness in the range 15–20 μm although there are gaps between the film and the substrate, and the films are extremely rough [26]. Diamond films grown from CH_4–Ar plasmas are able to form directly on SiO_2 substrates without the need for damaging the SiO_2 layer since the gas phase carbon dimer species in the UNCD process

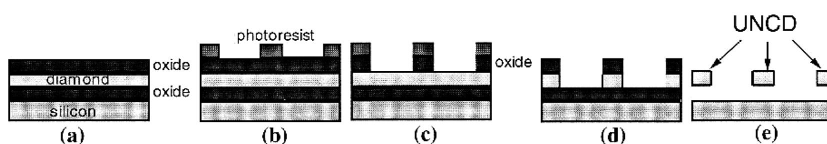

Figure 3. A schematic diagram showing lithographically based microfabrication of UNCD MEMS: (a) deposition of UNCD on the SiO_2 sacrificial layer plus masking layer; (b) and (c) the photoresist and lithography; (d) reactive ion etching in oxygen plasma; (e) selective chemical etching of SiO_2 sacrificial layer.

(a) (b)

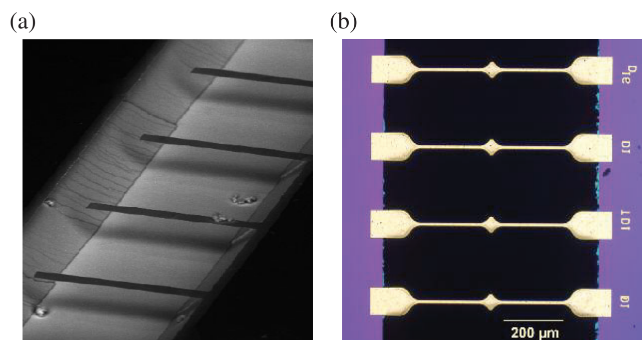

Figure 4. UNCD cantilevers (a) and membranes (b) produced by the fabrication method shown in figure 3.

forms an intermediate SiC nucleation layer via the reaction

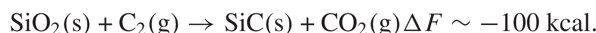

$$SiO_2(s) + C_2(g) \rightarrow SiC(s) + CO_2(g) \Delta F \sim -100 \text{ kcal}.$$

It is therefore possible to use SiO_2 as a sacrificial substrate layer for multilayer UNCD devices. As shown in figure 3(a), a UNCD layer is deposited on a thermal SiO_2 layer, followed by a second SiO_2 layer being deposited by CVD. Photoresist (b) is then used to pattern the hard SiO_2 mask using RIE with a CF_4/CHF_3 (2:1) plasma (c). An oxygen plasma is then used to etch the UNCD film through the hard SiO_2 mask. Initial measurements of etch rate, although not optimized, indicate that UNCD can be etched with a rate of about 1 μm h^{-1}. This number may change when better measurements are made. Finally, an HF wet and/or gas etch (d) is used to remove the sacrificial oxide layer, leaving the diamond film suspended above the Si substrate.

Figure 4 shows cantilevers and membranes produced by the method of figure 3 to measure mechanical properties at the MEMS scale.

The microfabrication technique shown in figure 3 was also used to produce a UNCD based microturbine–shaft integrated MEMS assembly suitable for microfluidic applications (figure 5).

Finally, in relation to how small the features that can be fabricated can be, we have recently produced 200 nm $\times$ 200 nm cantilevers, using a focused ion beam (FIB) etching method. At the present time, we do not know whether we can fabricate smaller features. However, considering that the grain size is 3–5 nm, in principle, it can be envisioned that features as small as 50–100 nm could be fabricated. Definitely, there are no other diamond films known today that can be patterned to such small dimensions, because of the grain size limitations: $\sim$1 μm for microcrystalline diamond and 30–100 nm for conventional nanocrystalline diamond films grown with the CH_4/H_2 plasma chemistry.

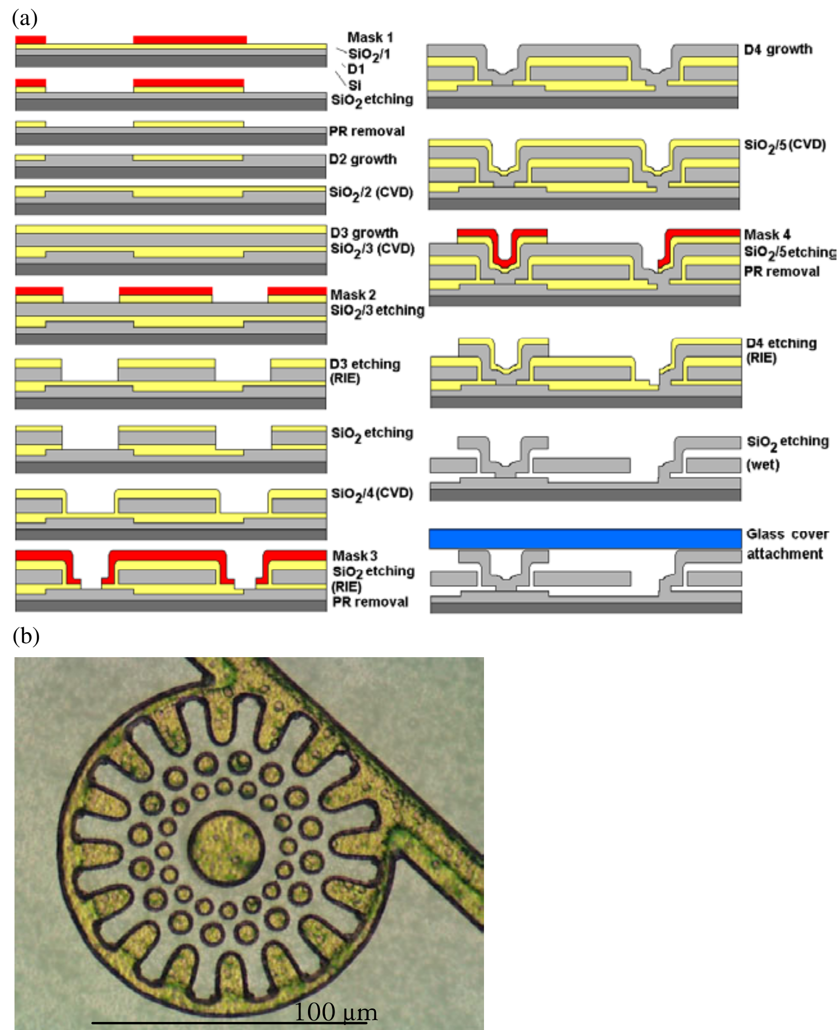

Figure 5. (a) A schematic diagram of the microfabrication process used to produce an integrated UNCD microturbine–shaft assembly; (b) an optical picture of the UNCD microturbine fabricated using the process shown in (a).

In addition to the two-dimensional UNCD MEMS structures shown above, we have also demonstrated the fabricability of three-dimensional structures as shown in figure 6.

5. Measurement of mechanical properties of UNCD at the MEMS scale

5.1. Membrane deflection experiment

We used a membrane deflection experiment (MDT), developed by Espinosa *et al* [27] as a novel microscale mechanical test for evaluating the elasticity, plasticity and fracture of thin films, to measure the mechanical properties of UNCD at the MEMS scale. The method works by stretching a free-standing, thin film membrane in a fixed–fixed configuration where the membrane is attached at both ends and spans a micromachined window beneath; see

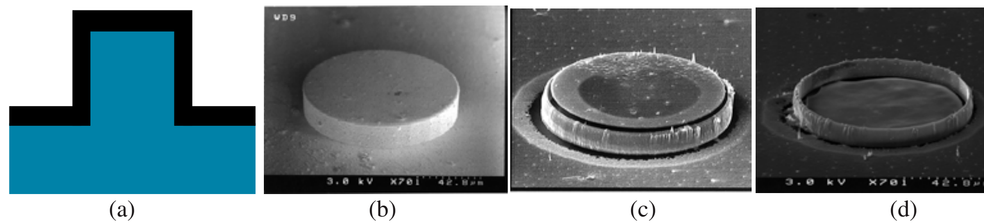

Figure 6. (a) A schematic diagram of a conformal UNCD coating on a Si post; SEM pictures of a UNCD-coated Si post (b), a UNCD-coated Si post after Ar ion bombardment to expose the edge, (c) after partial selective chemical etching of the Si core and (d) after total etching of the Si core producing a three-dimensional UNCD ring structure.

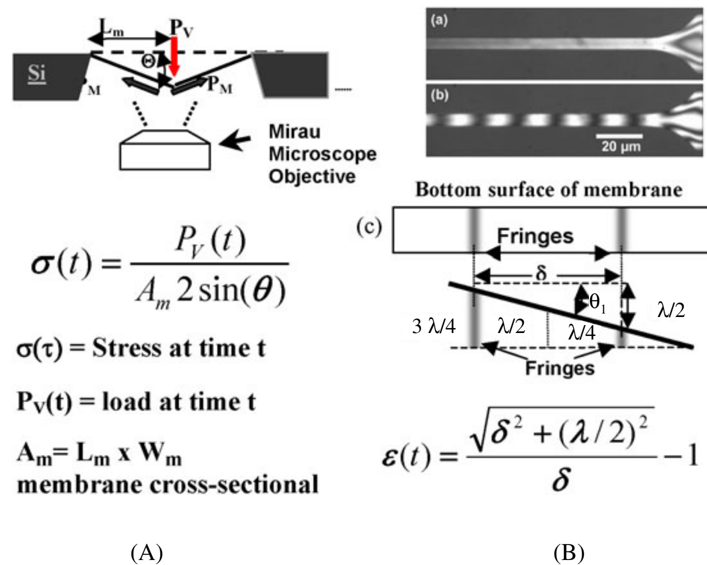

Figure 7. (A) A schematic diagram of the MDT method showing the load P_v applied to a UNCD membrane and the membrane in-plane load P_{m}, and an analytical expression that allows calculation of the Cauchy stress; (B) monochromatic images of an unloaded (a) and loaded (b) UNCD membrane that developed fringes; (c) a schematic representation of distance between fringes (δ) and the vertical displacement induced by the load.

figure 4(b) above. A nanoindenter applies a line-load at the centre of the span to achieve deflection. Simultaneously, deflection is recorded by the nanoindenter displacement sensor or by an interferometer focused on the bottom of the membrane through-view window in the wafer (see figure 7). The geometry of the membranes is such that it contains tapered regions eliminating boundary failure effects. The basic architecture can be described as double-dog-bone. The result is direct tension, in the absence of strain gradients, of the gauged region. These measurements provide quantitative information on mechanical properties such as the Young's modulus, residual stress state and yield and/or fracture stress. The data reduction for the membrane deflection tests (MDT) was explained in detail by Espinosa *et al* [27], and detailed measurements on UNCD membranes were presented in one of our prior publications [28]. A brief summary is given here. The procedure involves applying a line-load, with a nanoindenter, at the centre of the spanning membrane. Simultaneously, an interferometer focused on the bottom of the membrane records the deflection. The result is direct tension in the gauged

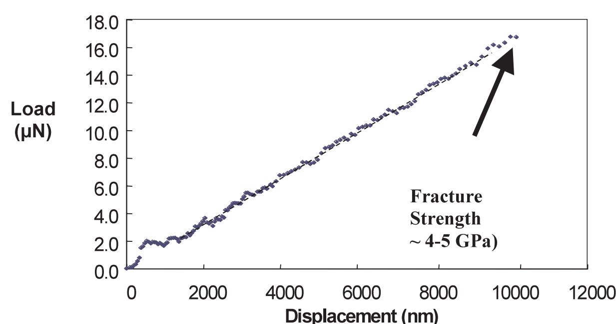

Figure 8. A load versus displacement curve for a UNCD membrane showing the fracture strength of the as-fabricated UNCD membrane.

regions of the membrane with load and deflection being measured independently. The data directly obtained from the MDT test must then be reduced to arrive at a stress–strain signature for the membrane. The Cauchy stress is obtained via the equation shown in figure 7(A), where the cross-sectional area of the membrane was measured with an AFM. The interferometer measurements as shown in figure 7(B) yield vertical displacement information in the form of monochromatic images taken at periodic intervals (see figure 7(B)). The relationship for the distance between interference fringes, δ, is through the wavelength, λ, of the monochromatic light used. By finding the average distance between the number of fringes that are in the focal plane of the interferometer, an overall strain, $\varepsilon(t)$, for the membrane can be computed from the relation shown in figure 7(B).

Several key experimental details were taken into account in order to obtain reliable results. For example, the UNCD membranes as originally released from the Si substrate were slightly bowed outward due the small residual stress of about 50–100 MPa, out of the wafer plane. Due to this effect, additional parameters were considered in the data reduction. This came in the form of identifying the height above the plane of the wafer where the tip makes contact with the membrane as well as the complete length of the membrane in its out-of-plane form. These are used to determine the deflection required before straining of the membrane begins. This part of the procedure consists of using interferometry to determine the height above the wafer plane where the tip makes contact with the membrane. The second step is to calculate the new half-length of the membrane based upon its out-of-plane curvature. From this point of contact in the test, the height of contact above the wafer plane (Δ_c) is added to the deflection. The deflection required before straining of the membrane begins (Δ_s) is also added to the deflection, which identifies the starting point of the stress–strain curve. Further details of this measurement can be found in [28]. As a summary of these measurements, figure 8 shows the fracture strength of UNCD as measured using the method described above.

Measurements were made on several membranes in order to get reliable statistical values. The response of the individual membranes was uniform from sample to sample with each exhibiting a statistical variation in failure point. The stress–strain response shown in figure 8 above exhibited a linear behaviour until failure occurred at about 4–5 GPa. This value is low considering that UNCD exhibits very high values for other mechanical properties shown below. We attribute this low fracture value to defects such as rugged edges of the membranes produced during etching and film surface roughness. We are now working on improving the surface roughness of the UNCD film and the microfabrication process to get smoother edges on the membranes to determine a more accurate value for the intrinsic fracture strength of UNCD.

5.2. Microcantilever deflection experiments

The cantilever deflection experiment was performed using different characteristic cantilever lengths (see the example of UNCD cantilevers shown in figure 4). A nanoindenter deflected the cantilever to a prescribed depth. Load and deflection were recorded by the nanoindenter. The raw data obtained from the tests were processed to obtain the desired quantities. For instance, in the cantilever tests the load obtained from the nanoindenter must be properly reduced to remove thermal drift and support spring stiffness of the nanoindenter components. This procedure has been described elsewhere [27]. The resulting load–deflection curve was then analysed for cantilever stiffness. The initial linear part of the curve was used to measure stiffness. The experimentally measured value of stiffness obtained from the load–deflection curves was used in conjunction with the standard stiffness equation for deflection of a uniform beam (equation (1)), with the plate modulus to account for the large width to length ratio:

$$k = \frac{Eb}{4(1-\nu^2)}\left(\frac{t}{l}\right)^3, \qquad (1)$$

where k is the stiffness, E is the elastic modulus, b is the cantilever width, ν is the Poisson ratio, t is the thickness and l is the length of the cantilever at the point of contact. However, since the Poisson's ratio for diamond is 0.07, the Poisson effect can be ignored and the equation becomes that of a uniform beam. From this equation, the elastic modulus of the material was determined to be about 937 GPa (very close to the value of 1000 GPa for single-crystal diamond). Further details of these measurements, including statistical analysis, are presented elsewhere [28].

5.3. Tribological behaviour of UNCD

Prior macroscopic tribological measurements, using the pin-on-disc method, performed in our laboratory [10], showed that UNCD exhibits coefficients of friction of about 0.02–0.04 in air. In addition, wear tests revealed that UNCD films exhibit practically no wear in extended tests. Obviously, these measurements need to be made at the MEMS scale. We are currently in the process of performing these measurements, and they will be reported in a separate publication.

6. Other properties of UNCD relevant to MEMS

We have recently demonstrated that we can achieve for the first time high electrical conductivity in n-type doped UNCD films via nitrogen doping [29]. We can tailor the electrical conductivity from an insulator to practically a semimetal ($\sim$166 W^{-1} cm^{-1}) depending on the amount of nitrogen incorporated in the UNCD films [29]. This unique electrical conduction seems to depend as much on the particular grain boundary structure and bonding, including nitrogen incorporation into the grain boundaries [30], as on the microstructural changes in nitrogen doped UNCD films that reveal grain size enlargement to $\sim$16 nm from the 2–5 nm characteristic of undoped UNCD, and grain boundary size increase from about 0.4 to 2.2 nm from undoped to doped UNCD [31]. The tailoring of the electrical conductivity of UNCD plays a critical role in the use of UNCD in MEMS devices that require electrical actuation such as RF MEMS switches and resonators, and we are currently performing research and development of such devices.

Another relevant property recently demonstrated by our group in collaboration with Professor Hamers [32] is that related to biofunctionalization of the UNCD film surface. In this recent work, Professor Hamers' group used a photochemically assisted process to chemically modify the hydrogen terminated UNCD surface of a film grown on a Si

substrate. The chemically modified UNCD surface consisted of a homogeneous layer of amine groups attached to the surface, on which DNA strands were chemically fixed. After linking DNA molecules to the amine groups, hybridization reactions with fluorescence tagged complementary and non-complementary oligonucleotides showed no detectable non-specific adsorption with extremely good selectivity between matched and mismatched sequences. Comparisons of the UNCD functionalized surface with other common surfaces used by other groups, such as gold, silicon, glass and glassy carbon, showed that diamond is unique in its ability to achieve very high stability and sensitivity as a functionalized surface in addition to being compatible with microelectronic processing technologies. Both processes open the way for biosensors based on UNCD, and we are pursuing this.

Finally, we are in the process of demonstrating that UNCD is biocompatible, which opens the way for the development of MEMS biodevices.

7. Conclusions

The tribological and mechanical properties of diamond make it in principle an ideal material for MEMS applications, particularly in harsh environments. However, the high intrinsic stress, rough surface and inappropriate grain morphology associated with conventional CVD deposition make most diamond films produced by this method unsuitable for use as MEMS material. We have developed a process for the growth of phase-pure ultrananocrystalline diamond films with mechanical and tribological properties that are well matched for MEMS applications. Fabrication methods, some of them related to those of Si fabrication technology and others unique to diamond, have been demonstrated in the fabrication of UNCD MEMS components. We have demonstrated the fabricability of 2D and 3D MEMS structures suitable for the fabrication of MEMS devices. Mechanical properties measured at the MEMS scale as well as macroscopic tribological measurements reveal that UNCD provides a superior material platform for MEMS. We have also demonstrated that UNCD can be doped with nitrogen resulting in high conductivity layers that open the way for electrically actuated MEMS such as RF switches and resonators. In addition, recent work demonstrated that UNCD surfaces can be functionalized to attach DNA and other biomolecules, opening the way for UNCD based biosensors. Finally, current work is showing that UNCD may be biocompatible, opening the way for MEMS biodevices.

Acknowledgments

This work was supported by the US Department of Energy, Office of Basic Energy Science, and Office of Transportation Technology, under contract W-39-109-ENG-38. This work was also sponsored by the National Science Foundation under Career Award No CMS-9624364 and under GOALI Award No N00014-97-1-0550, and supported in part by the Nanoscale Science and Engineering Initiative of the National Science Foundation under NSF Award Number EEC-0118025 and by DOE-Office of Science under contract No N00014-97-1-0550. Special thanks are due to W Oliver and B Peters of MTS Systems Corporation for their assistance in the utilization of the nanoindenter during this investigation.

References

[1] Sniegowski J J 1998 *Tribology Issues and Opportunities in MEMS* ed B Bushan (Netherlands: Kluwer–Academic) p 325

[2] Gabriel K J, Behi F, Mahadevan R and Mehregany M 1990 *Sensors Actuators* A **21–23** 184

[3] Lee A P, Pisano A P and Lim M G 1992 *Mater. Res. Soc. Symp. Proc.* **276** 67
[4] Gardos M N 1998 *Tribology Issues and Opportunities in MEMS* ed B Bushan (Netherlands: Kluwer Scientific) p 341
[5] Breuer K 2000 Challenges for lubrication in high speed MEMS *Nanotribology: Critical Assessment and Research Needs* (Netherlands: Kluwer Scientific) at press
[6] Tong L, Mehregany M and Matus L G 1992 *Appl. Phys. Lett.* **60** 2992
[7] Gardos M N 1999 Thinning films and tribological interfaces *Proc. 26th Leeds–Lyon Symp. on Tribology (Leeds, UK, Sept. 1999)* (Amsterdam: Elsevier)
[8] Rymuza Z, Kusznierewicz Z, Misiak M, Schmidt-Szalowski K, Rzanek-Boroch Z and Sentek J 1998 *Tribology Issues and Opportunities in MEMS* ed B Bushan (Netherlands: Kluwer–Academic) p 579
[9] Gardos M N 1999 *Surf. Coat. Technol.* **113** 183
[10] Krauss A R, Auciello O, Gruen D M, Jayatissa A, Sumant A, Tucek J, Mancini D, Moldovan N, Erdemir A, Ersoy D, Gardos M N, Busmann H G, Meyer E M and Ding M Q 2001 *Diamond Relat. Mater.* **10** 1952–61
[11] Erdemir A, Bindal C, Fenske G R, Zuiker C, Csencsits R, Krauss A R and Gruen D M 1996 *Diamond Films Technol.* **6** 31
[12] Spitsyn B V, Bouilov L L and Derjaguin B V 1981 *J. Cryst. Growth* **52** 219
[13] Kohn E, Gluche P and Adamschik M 1999 *Diamond Relat. Mater.* **8** 934
[14] Gruen D M, Liu S, Krauss A R, Luo J and Pan X 1994 *Appl. Phys. Lett.* **64** 1502
[15] Birrell J, Carlisle J A, Auciello O, Gruen D M and Gibson J M 2002 *Appl. Phys. Lett.* **81** 2235
[16] Jiao S, Sumant A, Kirk M A, Gruen D M, Krauss A R and Auciello O 2001 *J. Appl. Phys.* **90** 118–22
[17] Zuiker C D, Krauss A R, Gruen D M, Carlisle J A, Terminello L J, Asher S A and Bormett R W 1996 *Mater. Res. Soc. Proc.* **437** 211
[18] Gruen D M, Krauss A R, Csencsits R, Zuiker C D, Carlisle J A, Jimenez I, Sutherland D G J, Terminello L J, Shuh D K, Tong W and Himpsel F J 1996 *Appl. Phys. Lett.* **68** 1640
[19] Keblinski P, Wolf D, Phillpot S R and Gleiter H 1998 *J. Mater. Res.* **13** 2077
Keblinski P, Wolf D, Cleri F, Phillpot S R and Gleiter H 1998 *Mater. Res. Soc. Bull.* **23** 36
[20] Ramesham R 1999 *Thin Solid Films* **340** 1
[21] Kulisch W, Malave A, Scholz W, Mihalcea C, Oesterschulze E and Lippold G 1997 *Diamond Relat. Mater.* **6** 906
[22] Davidson J L, Ramesham R and Ellis C 1990 *J. Electrochem. Soc.* **137** 3206
[23] Dorsch O, Holzner K, Werner M, Obermeir E, Harper R E, Johnston C, Chalker P R and Buckley-Golder I M 1993 *Diamond Relat. Mater.* **2** 1096
[24] Givargizov E I, Zhirnov V V, Kuznetsov A V and Plekhanov P S 1993 *Mater. Lett.* **18** 61
[25] Irwin M D, Pantano C G, Gluche P and Kohn E 1997 *Appl. Phys. Lett.* **71** 716
[26] Chen C F, Chen S H, Hong T M and Tsai M H 1995 *J. Appl. Phys.* **77** 941
[27] Espinosa H D, Prorock B C and Fischer M 2003 *J. Mech. Phys. Solids* **51** 47–67
[28] Prorok B C, Espinosa H D, Peng B, Kim K-H, Moldovan N, Auciello O, Carlisle J A, Gruen D M and Mancini D C 2003 *Exp. Mech.* **43** 256–68
[29] Battacharyya S, Auciello O, Birrell J, Carlisle J A, Curtiss L A, Goyete A N, Gruen D M, Krauss A R, Schlueter J, Sumant A and Zapol P 2001 *Appl. Phys. Lett.* **79** 1441–3
[30] Zapol P, Sternberg M, Curtiss L A, Frauenhein T and Gruen D M 2002 *Phys. Rev.* B **65** 45403
[31] Birrell J, Carlisle J A, Auciello O, Gruen D M and Gibson J M 2002 *Appl. Phys. Lett.* **81** 2235–7
[32] Yang W, Auciello O, Butler J E, Cai W, Carlisle J A, Gerbi J E, Gruen D M, Knickerbocker T, Lasseter T, Russell J N, Smith L M and Hamers R J 2002 *Nat. Mater.* **1** 253–7